MODELLING OF LIGNIN THERMOLYSIS [+]

M.T. Klein* and P.S. Virk

Department of Chemical Engineering
Massachusetts Institute of Technology, Cambridge, MA 02139

Introduction

The object of the present work was to attempt a fundamental description of lignin thermolysis. This was motivated by a recognition that the increased use of biomass and low-rank coal resources must be accompanied by an enhanced understanding of the factors which influence their thermal processing. Since lignin is a major component of biomass, and has a direct evolutionary linkage to peat and lignitic coals, insights into its thermolysis should prove relevant to the practical pyrolyses of both biomass and coal.

Our investigation comprised three major components. First, a critical examination of lignin structure and chemistry was undertaken to discern the most likely thermolysis reaction pathways. Second, based on the foregoing, model compounds mimicking the essential reactive moities in the lignin substrate were selected and pyrolysed. Third, and finally, reaction pathways suggested by the model compound studies were coupled with a structural analysis of lignin to formulate a mathematical model which simulated the essential features of lignin thermolysis. The present paper will focus on the modelling of lignin thermolysis; a special effort is made to compare our model results with experimental data from lignin thermolyses previously reported in the literature.

In outline of what follows, our approach to the problem is described first. This includes an analysis of lignin structure; the choice of model compounds with a summary of their experimentally-ascertained pyrolysis pathways; and the logic and mathematics of the lignin thermolysis simulation. Representative results are presented next, the simulated lignin thermolyses being described by the time-evolution of products, including gases, aqueous liquids, phenolic tars, and residue (char). We conclude with a discussion wherein the results of our simulation are compared with experimental data reported in the literature for each of the foregoing product fractions.

Lignin Structure

Lignin is a natural phenolic polymer formed by an enzyme-initiated random free-radical co-polymerization of coniferyl, sinapyl and coumaryl alcohol monomers. The available information concerning lignin structure is best summarized in Freudenberg's (1) classic depiction of "a representative portion of spruce lignin", shown in Figure 1, which was the starting point for the present investigation. Freudenberg's formula should not be interpreted as a literal chemical structure for lignin but rather as a schematic depiction of the bond types and proportions found therein by experiments (1, 2, 3).

Analysis of Freudenberg's formula led to its characterization along the following lines. Each aromatic unit, arising from a monomer, possesses in general a set of propanoid (3-carbon-atom) and methoxy-phenol substituents. These aromatic units are connected by eight types of interunit linkages. The most prevalent linkage is the β-etherified guaiacyl glycerol moiety, as occurs between the methoxyphenol of

*Present Address: Department of Chemical Engineering
University of Delaware, Newark, DEL 19711

[+]This work was supported by seed funds from the MIT Energy Laboratory.

unit 6 in Figure 1. Other linkages found, in descending frequency of occurrence, are α-ether (units 3-4), diphenylmethane (units 2-3), diphenylether (units 6-7), biphenyl (units 9-10), pinoresinol (units 8-9), and phenylcoumaran (units 17-18). An essential feature of lignin structure is that the propanoid and methoxyphenol substituents on a given aromatic unit are essentially independent of one another since they are never involved in bonding with each other. Thus, the probability that an aromatic unit should contain a propanoid substituent of type k and a methoxyphenol of type j is the product of the individual probabilities of the occurrence of k and j, as given in Figure 1.

The foregoing probabilistic interpretation of Freudenberg's lignin formula is reduced to an aromatic unit matrix $\underline{A}$ in Figure 2. Each matrix element a_{jk} represents the number of aromatic units which possess type j methoxyphenol and type k propanoid substituents. Each row of the matrix represents a specific methoxyphenol found in lignin; these can originate from each of the three lignin monomers and within these the phenolic moiety may either be free or etherified in any of four forms, namely phenethylphenylether, benzylphenylether, phenylether and phenylcoumaran. Each column of the matrix represents a 3-carbon-atom propanoid side chain, respectively guaiacyl glycerol(β-ether, αβ-ether, α-phenyl β-ether), phenyl hydroxy acetone, cinnamaldehyde, pinoresinol, conidendrinoidlactone, and phenylcoumaran.

The matrix $\underline{A}$ of Figure 2 serves three purposes. First, the chemical moieties contained in its rows and columns are the basis for selection of model compounds relevant to lignin thermolysis. Second, the numerical values of each element offer a concise probabilistic description of the lignin substrate. (Note, incidentally, that the present A-matrix refers to the prototypical spruce lignin described by Freudenberg's formula; in the more general case, $\underline{A}$ will be a function of lignin origin.) Third, as we shall shortly find, lignin thermolysis generally leaves aromatic units intact while altering the substituents; a natural extension of the A-matrix to account for all possible products from thermolysis of the moieties in its rows and columns can then be used to unambiguously chronicle lignin thermolysis in terms of the substituents associated at any time with each of the original (conserved) aromatic units of the lignin substrate.

Model Pathways

Model compounds selected to mimic the thermal reactions of lignin are listed in Table 1. For each entry, the table lists an abbreviated name, chemical structure, the aspect of lignin structure modelled, and experimental pyrolysis conditions of temperature, holding time, and initial concentration. It can be verified that the entries in Table 1 model most of the interunit linkages (IL), methoxyphenol substituents (MP), and propanoid chains (PC) which appear in Figure 1. Specifically, PPE models the β-ether linkage most prevalent in lignin; guaiacol models the methoxyphenol substituent associated with coniferyl alcohol which is the dominant monomer in spruce lignin; veratrole models an etherified methoxyphenol; cinnamyl alcohol models a propanoid chain substituent, as do cinnamaldehyde, iso-eugenol, and acetophenone. Note also that some of the compounds in Table 1 were chosen to model moieties which, while not originally present in lignin, arise during its thermolysis; for example, saligenol models a propanoid enol moiety resulting from the primary reversion of a guaiacyl-glycerol β-ether. Still other compounds in Table 1, such as anisole, served as controls in the mechanistic interpretation of the model pyrolyses.

Results of the model compound pyrolyses are summarized in Table 2. For each substrate, the table delineates the observed pyrolysis pathways, their associated products, and reaction kinetics. Primary pathways are designated with an R while secondary pathways, involving reactions of a primary product, are designated with an S. Reaction kinetics are described by Arrhenius parameters ($\log_{10}A(s^{-1})$, E*(kcal/mol)) for pseudo-first order reaction; actual reaction orders, where experimentally ascertained, are quoted in the final column of the table. As an example, in entry 1, PPE decomposes by primary reaction R1 to phenol and styrene

products; the associated Arrhenius parameters are (11.1, 45.0) and the reaction was experimentally found to be first order in PPE; further, the styrene product of R1 undergoes secondary reaction S1 to form ethyl benzene, toluene, and benzene. The data presented in Table 2 now permit a quantitative description of reaction pathways and kinetics in lignin thermolysis.

Simulation of Lignin Thermolysis

The logic employed in our simulation of lignin thermolysis is depicted in Figure 3. Consider first some typical transformations experienced by a lignoid aromatic unit as shown in Figure 3a. Initially (time t = 0), this unit I will be recognized as element a_{11} of the spruce lignin matrix $\underline{A}$. During thermolysis, suppose the propanoid chain of I is sequentially subjected to β-ether reversion, pathway R1:PPE in Table 2, and enol product dehydration, by pathway R1:SAL in Table 2. At some time t_1, then, the substrate I will, in part, be transformed to the intermediate product II with concurrent evolution of water. However, II can further react by parallel pathways R1:CAD and R1:GUA, respectively leading to propanoid chain decarbonylation and methoxyphenol demethanation; thus at some further time t_2, II will, in part, be transformed to III, with concurrent evolution of carbon monoxide and methane. It should be noted that in Figure 3a, the original aromatic ring remains intact while its propanoid chain and methoxyphenol substituents are variously altered, chronicling the course of thermolysis. In mathematical terms, each substituent contained in the original $\underline{A}$ matrix gives rise to a new set of substituents that represent its thermolysis according to the pathways given in Table 2. At any time, the contents (aromatic units) of the original element a_{jk} of $\underline{A}$ are conserved while being redistributed into the elements p_{mn} of a new $\underline{P}$ (product)-matrix which represents all possible substituents that can arise from the original set. A little reflection will show that $\underline{A}$ is really a submatrix (the top left corner, say) of $\underline{P}$. Some further detail into the nature of the $\underline{P}$-matrix, and the methods for product accounting, is given in Figure 3b. Consider the coniferaldehyde unit II in lignin, undergoing thermolysis. In Figure 3a, for simplicity, this was shown to react by two parallel pathways; however, in practice, it will undergo all possible reactions accessible to its methoxyphenol and propanoid chain substituents. Since these substituents are independent, the products will be formed by a superposition of the type shown in Figure 3b. The methoxyphenol in II is modelled by guaiacol A, which can pyrolyse by pathways R1: GUA and R2: GUA of Table 2 to catechol B and phenol C. The propanoid chain in II is modelled by cinnamaldehyde D which can pyrolyse by R1: CAD to styrene E. Thermolysis of II will then form all of the products shown in Figure 3b (and their associated gases), in amounts commensurate with the kinetics of the pathways involved.

The foregoing chemical logic was employed to mathematically simulate a constant volume batch pyrolysis of lignin. In this simulation, a set of differential equations, which described the time-variation of aromatic unit substituents, were solved numerically from an initial condition representing Freudenberg's spruce lignin. The rate of change of a given substituent was, in general, proportional to all other substituents, so that:

$$\text{Differential Equations:} \quad dX/dt = \underline{K}X; \quad dY/dt = \underline{L}Y \tag{1}$$

$$\text{Initial Condition:} \quad X = X_0, \; Y = Y_0 \text{ at } t = 0 \tag{2}$$

In these the vector X represents all methoxyphenol-related substituents while vector Y represents propanoid chain-related substituents; these are, respectively, the rows and columns of the product matrix $\underline{P}$. The matrices $\underline{K}$ and $\underline{L}$, derived in large part from Table 2, respectively contain the kinetic rate constants of those chemical reactions producing the components of vectors X and Y. The initial values X_0, Y_0 coincide with the sums of each row and column in the matrix $\underline{A}$, depicting the lignin substrate. Values of the vectors X and Y at any subsequent time t are a consequence of all possible chemical transformations embodied in the matrices $\underline{K}$ and $\underline{L}$. The contents of an element p_{mn} of the product matrix P then show the number of aromatic

units with methoxy-phenol related substituent m and propanoid chain-related substituent n. The nature of substituents m and n further permits the classification of product p_{mn} as either tar (single-ring aromatic unit) or residue (multiple aromatic rings). Details of the simulation logic, mathematics, and numerical evaluation are available (4).

Results

Thermolysis of the prototypical spruce lignin of Figure 1 was simulated at temperatures of 300, 400, 500, and 600C to holding times of 10^4, 10^4, 10^2, and 10^1 seconds, respectively. Representative results at 500C are presented in Figure 4, an arithmetic plot of product yield, expressed as weight percent of original lignin substrate, versus time. Four product fractions, namely, gas, aqueous liquids, phenolic liquids and carbonaceous residue, will be considered.

In regard to gas evolution, the simulation accounts for methane and carbon monoxide. In the uppermost section of Figure 4 it can be seen that both gases evolve fast initially and then more slowly, attaining asymptotic yields of circa 6 wt %, with methane slightly exceeding CO. The methane arises primarily from guaiacy types of methoxyphenol moieties, both those which are initially present with a free hydroxyl and those which arise by reversion of etherified hydroxyls. The CO originates both from the decarbonylation of carbonyl-containing propanoid chains and, to a lesser extent, from the demethoxylation of methoxyphenols. An account of these dual sites for CO release possessing quite different activation energies relative to the sites for CH_4 release, the simulation predicts that the ratio of CO/CH_4 should be >1 at low temperatures and conversions, <1 at moderate temperatures and conversions (as in Figure 4), and then again >1 at high temperatures.

Among aqueous liquids, the simulation accounts for water and methanol. As seen in the second (from top) section of Figure 4, the water yield increases monotonically, but with decreasing slope, to an ultimate value of $\sim$5 wt %. The water arises from two sources; predominantly it is formed from dehydration of enol units which result after β-ether reversion; minor amounts also arise from degradation of cinnamyl-alcohol types of propanoid chains. The ultimate methanol yield predicted is only about 0.1 wt %. This rather small value comes about because, in the simulation, methanol arises solely from cinnamyl alcohol moieties, which are relatively rare in lignin; further, the methanol-forming pathway is itself relatively minor amongst cinnamylalcohol pyrolysis pathways.

The phenolic liquids fraction of our simulated lignin thermolysis included some fifty individual phenolic compounds. The formation versus time for two sets of phenolic products is shown in the two lowest sections of Figure 4. In the upper of these two sections, it can be seen that the guaiacol production increases initially, reaches a maximum, and then decreases towards zero at long times; the catechol production increases slowly at low times but more strongly at longer times; phenol production increases monotonically with increasing time but always remains less than catechol. Qualitatively the same behavior is exhibited in the lowest section of Figure 4 by methylguaicol, methylcatechol, and para-cresol products, each of which is the methyl-substituted analogue of the preceding products; note however that yields of the methyl-substituted phenols are almost an order of magnitude higher than those of their unsubstituted homologues. Phenolic product trends seen in Figure 4 arise from the following considerations. The guaiacyl moiety occurs directly in lignin, and further arises from reversion of etherified methoxy-phenols; associated with these guaiacyl units are various propanoid chains, also subject to degradation. Thus coniferaldehyde and guaiacyl vinyl ketone are the most nearly primary guaiacol products, degrading to vinyl guaiacol, and hence to ethyl-, methyl-, and unsubstituted guaicol. Further, each guaicyl moiety is capable of demethanation and demethoxylation, which respectively yield the corresponding catechol and phenol. Each guaiacol product thus possesses pathways for formation and destruction, resulting in the characteristic yield maxima seen in Figure 4. From the foregoing, catechols

are seen to be secondary products, arising from guaiacyl moiety demethanation; this causes their initial production to be slow but at long times they become the dominant phenolic products. Finally, phenols arise from two major sources, namely guaiacyl demethoxylation, noted above, and coumaryl alcohol monomer units directly incorporated in the lignin; the former source being of greater import. Phenol substitution patterns parallel those of guaiacol, with alkyl side-chains ranging from coumaraldehyde to vinyl-, ethyl-, and unsubstituted phenol. Yields of phenols relative to catechols increase somewhat with increasing temperature, since guaiacyl demethoxylation is more highly activated than guaiacyl demethanation; however the absolute yields of phenols always remained lower than those of catechols.

According to our simulation, the carbonaceous residue is comprised of all aromatic units involved in interunit bonding. If the gas, aqueous liquid, and phenolic product fractions are designated as volatile, and all multiple ring aromatics as non volatile, then the simulated carbonaceous residue fraction can be related to the weight loss that would be observed during lignin thermolysis. Such simulated weight-loss versus time curves are shown by the dashed lines in Figure 5, which will be more fully discussed in the next section.

Discussion

The discussion will be confined to comparisons between the present results and previous literature, as embodied in the matrix of Table 3. In the rows of this matrix, the four major product fractions have been delineated in terms of overall and constituent component yields. The matrix has six columns, representing our model predictions and five sets of literature references. The latter includes the collected reports of several authors as summarized in reference 4, the data of Iatridis and Gavalas (5), of Kirshbaum (6), and of Domburg (7, 8). In each matrix element, a numerical value or comment indicates that information relevant to that row was reported, whereas an 'X' implies that it was not. The present simulation column 1, provides entries for each row save CO_2 yield. The overall gas fraction is the sum of CO and CH_4; these are by far the prevalent constituents of the lignin off-gas. The aqueous distillate was composed of water and methanol only; acetone, acetic acid and other minor liquid products were not included in the simulation. The phenolic fraction comprised the sum of all single ring phenols; this overall yield should correspond best to the overall tar yield reported in pyrolysis experiments. Finally, the carbonaceous residue fraction is composed of all multiple ring aromatic units. The investigations of collected authors (4), column 2, provide detailed accounts of gas and aqueous distillate yields, and overall tar and char yields. Because detailed temperature-time information is lacking for many of these investigations, entries in this column are best considered the asymptotic 'ultimate' yields of destructive distillations. The data of Iatridis and Gavalas (5) were obtained in a reactor designed to emphasize primary reactions, providing detailed temperature-time information and entries for all save water and overall aqueous distillate yields. Kirshbaum (6) provided overall gas, phenolics, and carbonaceous residue yields; detailed phenolic product spectra were provided also. Detailed description of phenolic product spectra and DTA/DTG weight loss data were given by Domburg (7, 8). The discussion to follow considers each row of Table 3; note that all yields are in weight percent of original lignin substrate.

The simulated overall gas fraction rose with increasing time and temperature and ultimately achieved a value of about 15% at 600 C. This compares favorably with the data of collected authors (4) in Table 3, where gas yields ranged from about 10-20%. Iatridis and Gavalas report an overall yield as high as 23% at 650 C, but this included 7.2% CO_2. As discussed below, this rather high CO_2 content may be due to their use of a Kraft lignin. Omitting CO_2, their overall gas yield is 16%, in good agreement both with the simulation and earlier literature. Additionally, Kirshbaum reports total gas (and losses) yield of ∿5% at 250 C and ∿18% at 600 C. The simulated (CH_4, CO) yields are respectively (6.0, 5.0) % at (500 C, 100s) and

(6.1, 9.0) % at (600 C, 7s); both these CH_4 and CO yields are in substantial agreement with the collected literature (4) which provides ultimate (CH_4, CO) yields of (7.0, 7.0) %. Simulated methane and CO yields both somewhat exceed those of reference 5, but, interestingly, these authors report that the experimental CO/CH_4 ratio varied from about 2.3 at 400 C to 0.88 at 500 C and 1.8 at 600 C, which closely accords with the behavior of this ratio in our simulation. This was earlier interpreted in terms of dual sites for CO release from lignin.

The simulated overall yield of aqueous liquids, based on the sum of water and methanol yields, was about 6%, appreciably lower than the average yields of ∿15% reported by the collected authors (4). Of the two individual components, the simulated water yields of 6% are about half of the values reported in the literature, although these latter are often unreliable on account of water being physically associated with the lignin or introduced during its isolation. Simulated methanol yields of 0.1% are also substantially lower than the yields of 0.28 to 1.5% reported by the collected authors (4). It would appear that further pathways for both water and methanol production need to be identified and incorporated into the present model of lignin thermolysis.

The simulated overall yield of phenolic liquids ranged from 7 to 80%. Experimental phenolic fraction yields typically range from 3 to 30% (4), although tar yields greater than 50% have been reported (9). The simulated phenolic fraction yields exceed experimental for two likely reasons. First, many complex phenols in the tar fraction are not experimentally identified and second, our simulation did not consider the condensation and polymerization reactions which might lower the yield of single ring phenols in practice. In regard to individual phenols, the present simulation predicts most of the thirty phenols which have been detected in the literature (6, 7, 8). In most cases, the simulated yields of individual phenols agree with experimental values to with a half an order of magnitude. It is particularly noteworthy that deviations between the present simulation and experiments are no greater than deviations between individual experiments.

The simulated carbonaceous residue yields of 91% at 300 C and 10^4s and 40% at 600 C and 7s compare favorably with the literature. In Table 3, ultimate tar yields from destructive distillation (4) were 40 to 60%. Iatridis and Gavalas (5) report weight losses of 20% and 53% at 400 and 600 C, respectively, corresponding to char yields of 80% and 47%. Kirshbaum (6) reports a char yield of 91% at 250 C and only 26% at 600 C. The present definition of residue as multiple ring aromatics evidently provides simulated carbonaceous residue yields that are in good accord with the experimental literature.

Finally, simulated weight-loss kinetics, derived from the carbonaceous residue yields as noted earlier, are compared with the experimental data reported by Iatridis and Gavalas (5) in Figure 5. It can be seen that the simulated weight loss curves (dashed), accord well with the experimental weight loss curves (solid), both in regard to shape and absolute magnitudes. The observed agreement is noteworthy in that the simulation was based entirely on our a priori description of lignin structure, reaction pathways, and kinetics, and incorporated no information derived from actual lignin thermolyses. Furthermore, the modest deviations between simulated and experimental weight loss curves in Figure 5 can reasonably be attributed to differences between the respective lignin substrates. The authors (5) used a Douglas for precipitated Kraft lignin, whereas the present simulation was based on Freudenberg's unperturbed "protolignin." Kraft pulping alters the chemical nature of lignin, resulting in increased internal condensations, with the original reactive α- and β-ether linkages transformed into less reactive diphenyl-methane, ethane, and ethylene linkages; it also introduces carboxylic acid units into the lignin macromolecule. The low temperature reactivity of a Kraft lignin might be expected to be greater than its protolignin counterpart because of facile CO_2 evolution from the carboxylic acid units. At higher temperatures and conversions, the reactivity of a Kraft lignin may well be lower than that of the protolignin since relatively re-

fractory diphenylmethane, ethane and ethylene units have replaced the original reactive α- and β-ethers. In the light of these assertions, it is interesting that Iatridis and Gavalas report CO_2 yields of 5.9% at 400 C and 120s, and 4.1% at 600 C and 10s. These suggest a constant number of easily decarboxylated acid sites in their substrate. Further, the authors' reported weight loss of 20% at 400 C and 120s exceeds our simulated weight loss of 13% by an amount substantially equal to their CO_2 yield. At 600 C and 10s the experimental weight loss corrected for CO_2 is ∿50%, somewhat lower than our simulated value of 60% on account of the reduced reactivity of their Kraft lignin.

Summary and Conclusions

Mathematical simulation of whole-lignin pyrolyses, at 300 to 600 C with holding times of 1 to 10^4s, was achieved by combining a statistical interpretation of lignin structure with experimental results of model compound pyrolyses. The outcome of these simulations, expressed in terms of product fractions as a percent of initial lignin was:

(i) Gas Fraction: Simulated overall gas, methane, and CO yields accorded with previous experimental lignin pyrolyses; respective ultimate yields typically 15%, 6%, and 9% were in quantitative agreement with the literature. The simulated variation of (CH_4/CO) ratio with time and temperature further agreed with that recently reported by Iatridis and Gavalas (5).

(ii) Aqueous Fraction: Simulated water yields were typically about half the reported experimental yields of 12%. Simulated methanol yields were half an order of magnitude lower than the literature yields of 0.3-1.5%.

(iii) Phenolic Fraction: Simulated overall phenolic liquids yields were generally higher than experimentally observed. The simulation accounted for more than thirty individual phenols reported in the literature. Simulated yields of simple individual guaiacols, cathechols, syringols, and phenols, each nominally 2%, were within the band of values reported in the literature.

(iv) Carbonaceous Residue: Simulated curves of weight loss versus time at 400, 500, and 600 C were nearly coincident with the experimental curves reported by Iatridis and Gavalas (5) for pyrolysis of a Kraft lignin. Also, the modest disagreements between these curves, at both low and high temperatures, were traced to structural differences between the respective lignin substrates.

References

1. Freudenberg, K., Neish, A.C., Constitution and Biosynthesis of Lignin, Springer-Verlag, New York (1968).
2. Harkin, J.M., in Battersby and Taylor, Oxidative Coupling of Phenols, Marcel-Dekker (1967).
3. Sarkanen, K.V., in Sarkanen, K.V., and Ludwig, C.H., eds., Lignins: Occurrence, Formation, Structure and Reactions, Wiley Interscience, New York, (1971).
4. Klein, M.T., Model Pathways in Lignin Thermolysis, Sc.D. Thesis, Department of Chemical Engineering, M.I.T., Cambridge, Mass. (1981).
5. Iatridis, B. and Gavalas, G.R., I & EC Prod. Res. Dev., 18 (2), 127 (1979).
6. Kirshbaum, I.Z., Domburg, G.E., Sergeeva, V.N., Khim. Dev. No. 4, 96 (1976).
7. Domburg, G.E., Sergeeva, V.N.,Kalnish, A.I., Thermal Analysis, Vol.3 (Proc. 3rd ICTA Davos (1971)) pp. 327-40, Burkhaeuser, Basel, (1972).
8. Domburg, G.E., Sergeeva, V.N., J. Thermal. Anal., 1, 53 (1969).
9. Domburg, G.E., Kirshbaum, I., Sergeeva, V.N., Khim, Dev. 7, 51 (1971).

TABLE 1. MODEL COMPOUNDS FOR LIGNIN THERMOLYSIS

	Compound	Abbr.	Structure	Model of	Pyrolysis Conditions T C	t s	C_0 mol/ℓ
1	Phenethyl-phenyl ether	PPE		IL	300-550	30-14400	0.083-1.68
2	Guaiacol	GUA		MP	250-535	110-6000	0.46-3.07
3	Veratrole	VER		MP	350-550	60-1500	0.33
4	Cinnamaldehyde	CAD		PC	250-400	120-1500	0.38-1.3
5	Saligenol	SAL		PC	175-350	60-1500	0.37
6	Cinnamyl-alcohol	CAL		PC	300-500	50-1500	0.37-1.1
7	2,6 Dimethoxy-phenol	DMP		MP	300-500	120-1600	0.32
8	Isoeugenol	IEG		MP,PC	300-500	60-1560	0.33
9	Vanillin	VAN		MP	300-500	120-1500	0.85
10	Acetophenone	APH	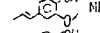	PC	350-550	120-5000	0.14-1.4
11	o-Hydroxy-diphenylmethane	OHD		IL	400-550	120-6000	0.27
12	Phenylether	PET		IL	500-587	240-9000	0.30
13	Cinnamic Acid	CIA		PC	250-400	120-1500	0.20
14	Ferulic Acid	FEA		PC,MP	200-350	120-1500	0.50
15	Anisole	ANI		CON	344-550	180-1500	0.46-3.07
16	Benzaldehyde	BAD		CON	300-500	120-3600	0.16-3.3

Note: Model codes are: IL - Interunit link, MP - Methoxyphenol, PC - Propanoid chain, CON - Control.

TABLE 2. MODEL PATHWAYS AND KINETICS IN LIGNIN THERMOLYSIS

	Substrate	Pathway:	Products	$\log_{10}A(s^{-1})$	E*(kcal/mol)	Order
1.	PPE	R1:	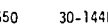	11.1	45.0	1
		S1:		5	22	(>1)
2.	GUA	R1:	CH_4 + 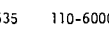	10.9	43.7	1
		R2:	CO + 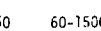	11.5	47.4	1
3.	VER	R1:	CH_4 + 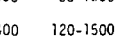	13.9	55.9	
		R1':	CO + CH_4 + 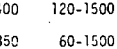	14.1	58.4	
		R2:	CO + 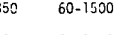	14.8	60.1	
		R3:	CO + 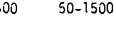	11.2	49.2	
4.	CAD	R1:	CO + 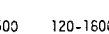	12.1	48.2	1
		R2:	Dimers	8.6	33.7	(2)
5.	SAL	R1:	H_2O +	13.4	33.4	(1)
6.	CAL	R1:	CAD	4.2	21.8	
7.	DMP	R1:	CH_4 + 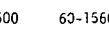	10.4	42.2	
		R2:	CO + 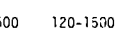	11.1	45.5	
8.	IEG	R1:	CH_4 + 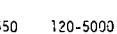	10.8	42.9	
		R2:	CO + 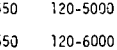	11.3	46.2	
9.	VAN	R1:	CH_4 + 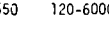	12.2	47.3	
		R2:	CO + 	10.2	38.5	
10.	APH	R1:	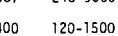 + CO	10.9	56.4	1
		R2:	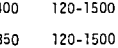	9.6	50.5	(1.5)
11.	OHD	R1:	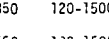 + 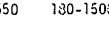	9.6	43.4	
12.	PE	R1:	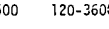 + 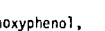	14.8	72.1	
13.	CAA	R1:	CO_2 + 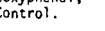	8.0	31.0	(1)
14.	FEA	R1:	CO_2 +	5.2	19.8	
15.	ANI	R1:	CH_4 +	13.0	54.7	1
		R2:	CO +	14.5	61.0	
		R3:		7.9	40.5	(1)
16.	BAD	R1:	CO +	9.5	41.5	1

Item	Model Prediction	Collected Authors: (4)	Iatridis and Gavalas (5)	Kirshbaum (6)	Domburg (7,8)
Gas Fraction					
Overall yields	15% @ 600C	10-20%, 15% mean	23% max including CO_2	5% @ 250C, 18% @ 600C gases and losses	X
CH_4	6% @ 600C	7% based on mean overall yield of 15%	4.8% @ 650C	X	X
CO	9% @ 600C	7% based on overall mean of 15%	9.2% @ 650C	X	X
CO_2	X not included in simulation	1.5%	near 6%, all temperatures	X	X
Aqueous Fraction					
Overall	6% maximum	overall mean 15%	X	X	X
H_2O	6% maximum	12-15%	X	X	X
MeOH	0.1% maximum	0.2-1.0%	3% @ 650C	X	X
Phenolic Fraction Overall	Sum of single ring phenols as function of time ; 7-80%, include complex phenols	3-30%	0.3-3.0%,400-650C	3.3-14.5%@475C	0.2%@250C, 14% @ 500C
Individual Phenols	Detailed yields of individual phenols as a function of time and temperature	X	only guaiacols and phenols	detailed yields of 20+ different phenols	detailed yields of 20+ different phenols
Carbonaceous Residue					
Overall	Ultimate residue yield from 0.914 @ 300C to 0.385 @ 600C	40-60% yield of char	weight loss of 20% @ 400C, 53% @ 600C	char yield of 91% @ 250C, 26% @ 600C	X
Kinetics	multiple ring aromatics as function of time, ultimate yields as function of temperature	X	weight loss for 400-600C as in function of time	X	DTA/DTG experiments yield E 26-30 kcal/mol

TABLE 3. COMPARISON BETWEEN LIGNIN THERMOLYSIS SIMULATION AND EXPERIMENTS.

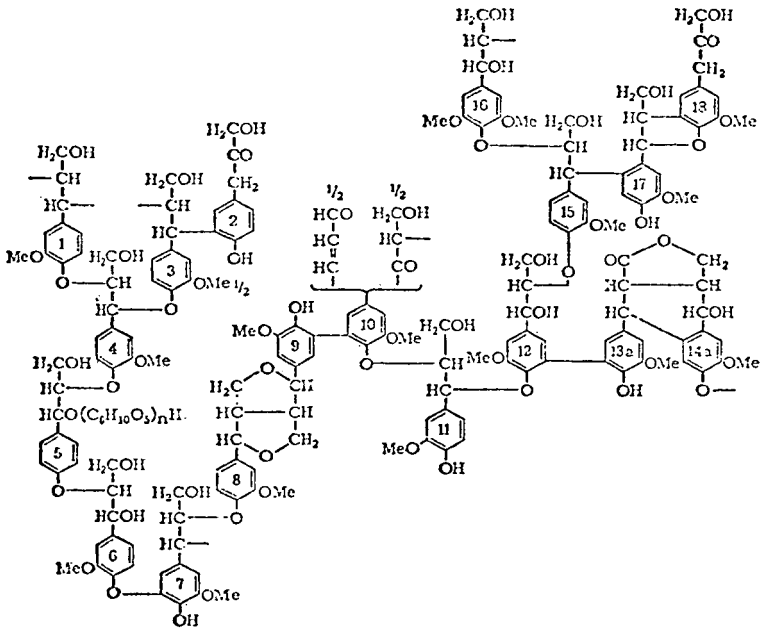

FIGURE 1. MODEL OF SPRUCE LIGNIN STRUCTURE (Freudenberg, 1)

MP \ PC										∑ MP
NORMALIZED DISTRIBUTION →		(.33)	(.11)	(.11)	(.11)	(.06)	(.11)	(.11)	(.06)	(1)
CONIFERYL ALCOHOL	FREE (.28)	1.66	.55	.55	.55	.30	.55	.55	.30	5
	ETHERIFIED (.56)	3.33	1.11	1.11	1.11	.60	1.11	1.11	.60	10
COUMARYL ALCOHOL	FREE (.055)	.327	.11	.11	.11	.060	.11	.11	.060	1
	ETHERIFIED (.055)	.327	.11	.11	.11	.060	.11	.11	.060	1
SINAPYL ALCOHOL	FREE (0)	0	0	0	0	0	0	0	0	0
	ETHERIFIED (.055)	.327	.11	.11	.11	.060	.11	.11	.060	1
∑ PC	(1)	6	2	2	2	1	2	2	1	18

FIGURE 2. AROMATIC UNIT MATRIX A FOR SPRUCE LIGNIN

FIGURE 3. LOGIC OF LIGNIN THERMOLYSIS SIMULATION.

(a) Thermal Transformation of Lignin Moiety.
(b) Superposition of Model Pathways.

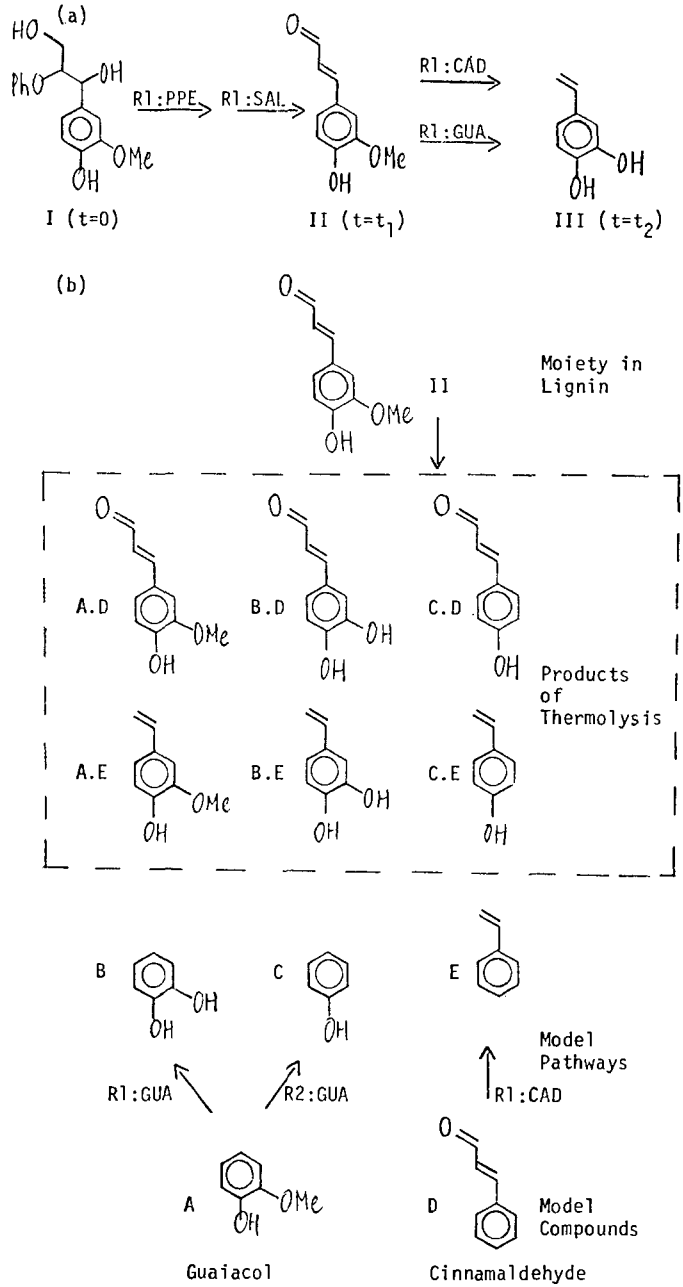

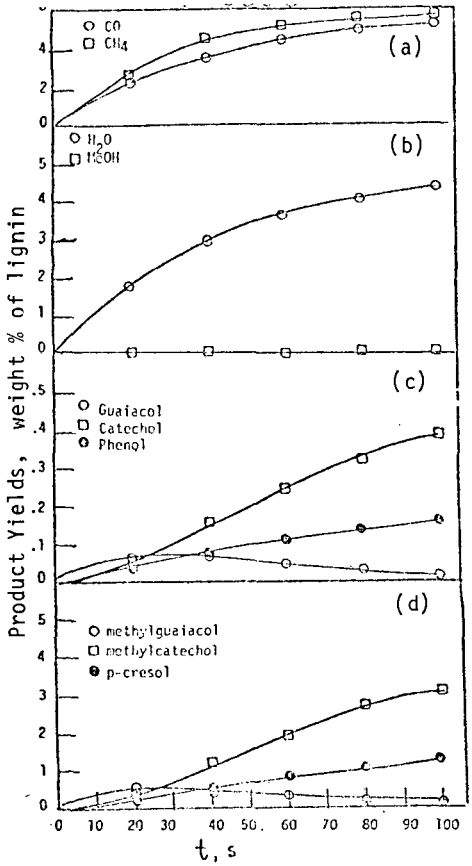

FIGURE 4. RESULTS OF LIGNIN THERMOLYSIS SIMULATION AT T = 500 C.

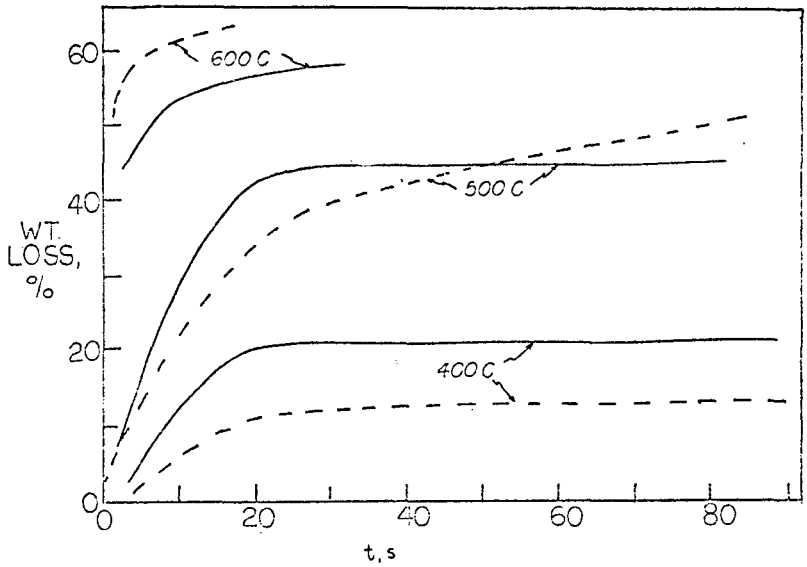

FIGURE 5. WEIGHT-LOSS KINETICS IN LIGNIN THERMOLYSIS.
—— Experimental (5)
- - - Present Simulation.